Supplementary Information (SI) for Nanoscale.

Supporting Information

3D Printing of Superhydrophobic and Multifunctional Objects via Simple and Inexpensive Vat Photopolymerization

Adil Majeed Rather,[a] Mohammed Barrubeeah,[a] Mohammad Javad Zarei,[a] Young Jae Kim,[a] Sravanthi Vallabhuneni,[a] Arun Kumar Kota*[a]

[a]Department of Mechanical and Aerospace Engineering, North Carolina State University, Raleigh 27695, USA

Corresponding author. Email: akota2@ncsu.edu

Section S1. Estimation of sliding angles

Based on a balance between work done by gravitational force and work expended due to adhesion, the sliding angle ω on a super-repellent surface is given as:

$$\rho g V \approx \gamma_{lv} D_{TCL}(\cos\theta^*_{rec} - \cos\theta^*_{adv}) \quad \text{(S1)}$$

Here, γ_{lv}, ρ and V are surface tension, density, and volume of the liquid droplet, respectively, and g is the acceleration due to gravity, θ^*_{adv} and θ^*_{rec} are the advancing contact angle and the receding contact angle, respectively, and D_{TCL} is the width of the triple phase contact line perpendicular to the sliding direction. When the shape of the droplet does not deviate significantly from a spherical cap, the width of the triple phase contact line can be computed as:

$$D_{TCL} = 2\sin\bar{\theta}^* \left[\frac{3V}{\pi(2-3\cos\bar{\theta}^*+\cos^3\bar{\theta}^*)}\right]^{\frac{1}{3}} \quad \text{(S2)}$$

Here, $\bar{\theta}^*$ is the average contact angle, given as:

$$\bar{\theta}^* = \frac{\cos\theta^*_{adv}+\cos\theta^*_{adv}}{2} \quad \text{(S3)}$$

The experimentally measured roll off angles of ~20 μL droplets of water are in reasonable agreement with those predicted using equations S1-S3 (see Tables S1 and S2).

Table S1. Measured and predicted sliding angles of water at different PVDF compositions. NS is no sliding.

PVDF (wt.%)	**Water**	
	ω (measured)	**ω (predicted)**
0	NS	NS
5	NS	NS
10	75°	64°
15	48°	43°
25	36°	34°
30	15°	12°
35	8°	6°

Table S2. Measured and predicted sliding angles of water at different washing times. NS is no sliding.

Washing Time (min)	**Water**	
	ω (measured)	**ω (predicted)**
0	NS	NS
15	65°	56°
30	38°	35°
45	18°	16°
60	8°	6°

Section S2. Cross-sectional surface morphology

We characterized the cross-sectional surface morphology of the (Figure S1a) and photopolymer resin + 35 wt.% PVDF (Figure S1b) after washing with acetone using SEM. In both cases, the cross-sectional morphology depicts the layer-by-layer 3D printing. However, the surface roughness of photopolymer resin + 35 wt.% PVDF (Figure S1b) is significantly higher than just the photopolymer resin (Figure S1a).

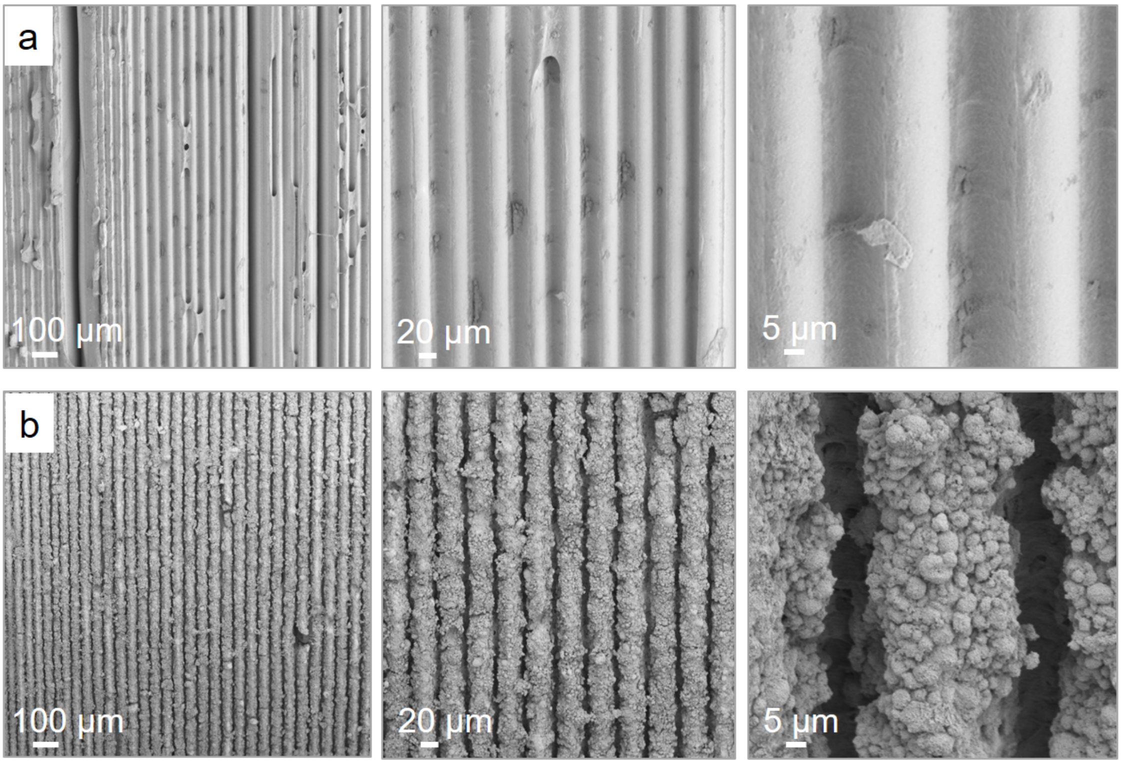

Figure S1. Cross-sectional surface morphology. Cross sectional SEM images of (a) photopolymer resin, and (b) photopolymer resin + 35 wt.% PVDF, after washing with acetone.

Section S3. FTIR characterization

Fourier transform infrared spectroscopy (FTIR) was used to characterize the chemical composition of different surfaces. FTIR spectra of photopolymer resin showed absorption peaks around 1156 cm^{-1}, 1728 cm^{-1} and 2900 cm^{-1}, indicating the presence of C=O, C-O-C and C-H bonds, respectively, of the acrylic ester groups (Figure S2a). FTIR spectra of PVDF showed absorption peaks around 796 cm^{-1}, 975 cm^{-1} and 1402 cm^{-1}, indicating the presence of α-phase of PVDF and around 878 cm^{-1}, 1072 cm^{-1} and 1170 cm^{-1}, indicating the presence of β-phase of PVDF (Figure S2b).

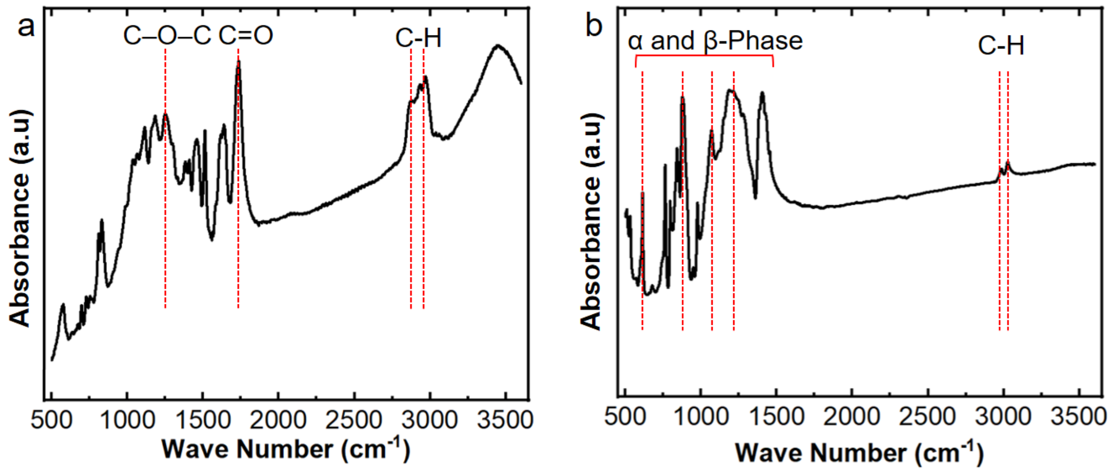

Figure S2. FTIR spectra. FTIR spectra of (a) photopolymer resin, and (b) PVDF particles.

Section S4. 3D printed complex shapes with superhydrophobic surfaces

We 3D printed a broad range of complex shapes with superhydrophobic surfaces, which is evident from water droplets (blue) beading up on the surface (Figure S3).

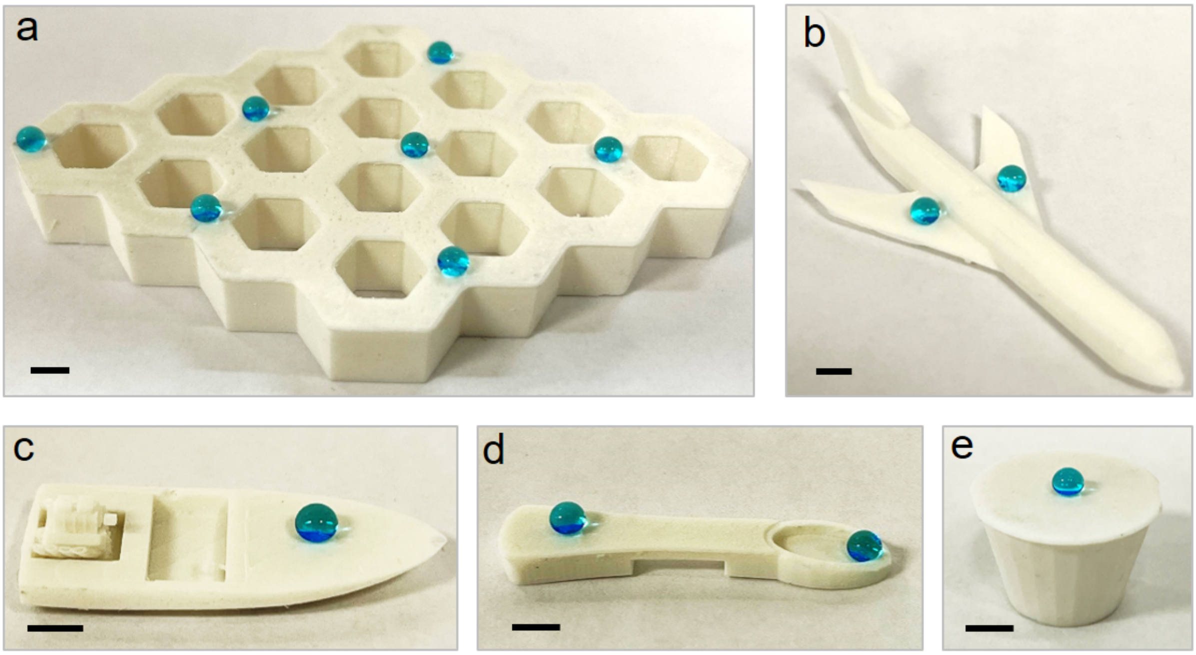

Figure S3. 3D printed superhydrophobic shapes. Droplets of water adopting the Cassie-Baxter state and beading up on various 3D printed superhydrophobic shapes including (a) honeycomb matrix, (b) aircraft, (c) boat, (d) spoon and (e) truncated cone. Scale bars represent 5 mm.

Section S5. Chemical resistance to aqueous corrosive liquids

To demonstrate the chemical resistance of our 3D printed superhydrophobic surfaces, we exposed them to aqueous corrosive liquids with different pH values for 1 h. The pH of the corrosive liquids was systematically varied from 7 to 1 by adding hydrochloric acid (Fisher) to water, and from 7 to 13 by adding sodium hydroxide (Fisher) to water. The contact angles and sliding angles of water on our 3D printed superhydrophobic surfaces remained virtually unaltered (Figure S4), indicating their chemical resistance.

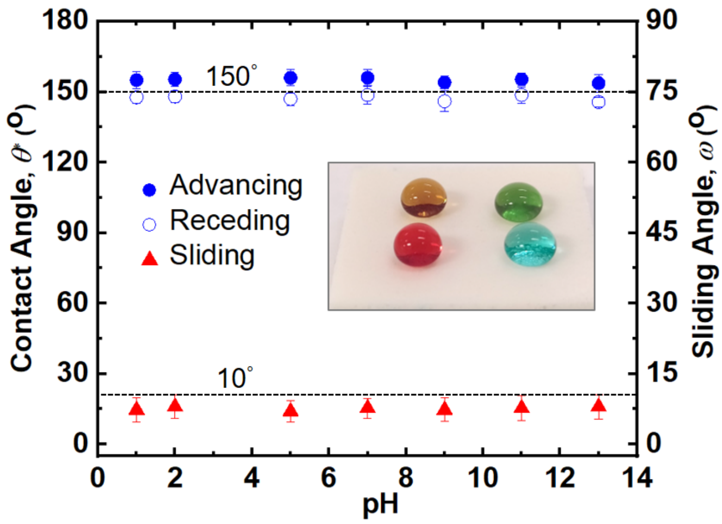

Figure S4. Chemical resistance of 3D printed superhydrophobic surfaces. Advancing and receding contact angles, as well as sliding angles of water on our 3D printed superhydrophobic surfaces after 1 h exposure to liquids with different pH values. Inset shows the droplets of aqueous liquids with pH = 1 (red), pH = 5 (dark brown), pH = 7 (blue), and pH = 13 (green), adopting the Cassie-Baxter state and beading up on our 3D printed superhydrophobic surfaces.

Section S6. Blade scratch resistance

To demonstrate the blade scratch resistance on our 3D printed superhydrophobic objects, we scratched the surface of our 3D printed object in arbitrary directions with a sharp edged knife. Next, we placed a water droplet (20 µL) on the scratched region of the 3D printed object. The water droplet displayed superhydrophobic property with high contact angle above 150° and sliding angle less than 10° even at the scratched region (Figure S5).

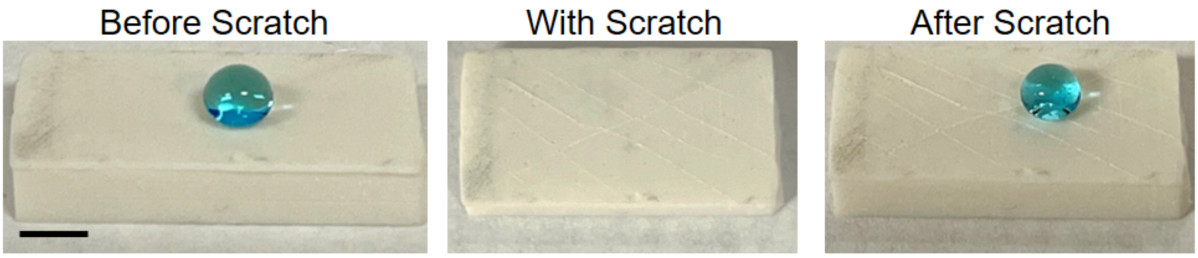

Figure S5. Blade Scratches on 3D printed objects. Images showing the water droplet beading on 3D superhydrophobic object before and after blade scratches. Scale bar represents 5mm.

Section S7. Mechanical properties of 3D printed objects

We measured the quasi-static mechanical properties of the 3D printed resin, resin + 35 wt% PVDF, and resin + 35 wt% PVDF + fluorinated Fe_3O_4 using ASTM Type I specimens in a tensile tester (Mark-10). A comparison of the stress-strain curves (Figure S5) and the Young's modulus and % strain to failure (Table S3) indicated that there is no significant difference in the mechanical properties before and after adding PVDF or fluorinated Fe_3O_4.

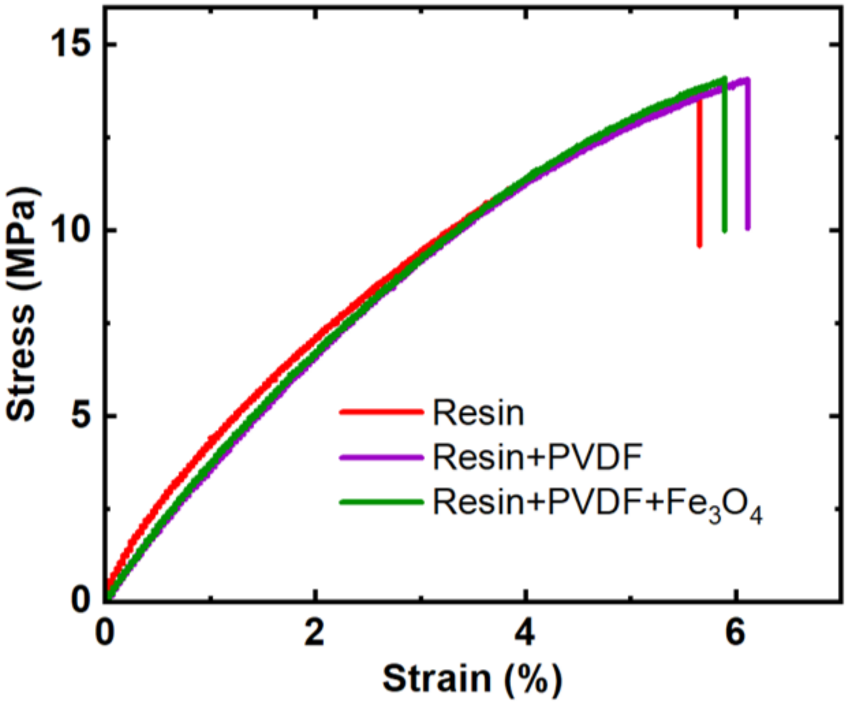

Figure S6. Mechanical properties of 3D printed objects. Stress-strain curves of resin, resin + 35 wt% PVDF and resin + 35 wt% PVDF + Fe_3O_4.

Table S3. Mechanical properties of resin, resin + 35 wt% PVDF and resin + 35 wt% PVDF + Fe_3O_4.

Sample Type	Young's Modulus (MPa)	Strain to Failure (%)
Resin	4.2±0.4	6.0±0.5
Resin + 35 wt.% PVDF	3.6±0.2	5.8±0.7
Resin + 35 wt.% PVDF + Fe_3O_4	3.5±0.3	5.5±0.6

Movie Legends

Movie S1. This video illustrates the separation of water (blue) and hexane (red; floating on water) using a 3D printed superhydrophobic porous cuboid, which completely absorbed hexane, but did not absorb any water.

Movie S2. This video illustrates the separation of water (blue) and chloroform (red; submerged in water) using a 3D printed superhydrophobic porous cuboid, which completely absorbed chloroform, but did not absorb any water.